STUDY ON THE DISTURBANCE EFFECT OF PULSATING FLOW AND HEAT TRANSFER IN SELF-EXCITED OSCILLATION SHEAR LAYER

by

Gaoquan HU [a,b], ***Zhaohui WANG*** [a,b*], ***Yiwei FAN*** [a,b], ***Hongmei YUAN*** [a,b], ***and Quanjie GAO*** [a,b]

[a] Key Laboratory of Metallurgical Equipment and Control Technology of Ministry of Education, Wuhan University of Science and Technology, Wuhan, China
[b] Hubei Key Laboratory of Mechanical Transmission and Manufacturing Engineering, Wuhan University of Science and Technology, Wuhan, China

Original scientific paper
https://doi.org/10.2298/TSCI210611347H

The fluid movement motion has an important influence on the evolution of the pulsating flow in the hot runner. Using the large eddy simulation numerical method, the instantaneous velocity, wall shear stress, boundary-layer thickness, and Nusselt number of hot runner section under different structural parameters at an inlet pressure of 5000 Pa were studied. The research results showed that the backflow vortex can be formed in the hot runner, and the fluid at the axis center of hot runner can form a pulsating flow under the squeezing action of the backflow vortex. The pulsating flow had a strong disturbance effect on the fluid around the axis center and accelerated the heat exchange between the fluid around the axis center and the wall. The disturbance effect of pulsating flow gradually strengthened with the flow of the main flow to the downstream. When d_2/d_1 *was 1-1.8, the wall shear stress first increased and then decreased, and the wall heat transfer efficiency first increased and then decreased. The maximum wall shear stress was 36.4 Pa. When L/D was 0.45-0.65, the boundary-layer thickness first decreased and then increased, and the heat transfer efficiency first increased and then decreased. The minimum boundary-layer thickness was 0.392 mm and the maximum Nusselt number was 138. When* d_2/d_1*=1.4 and L/D=0.55, the maximum comprehensive evaluation factor reached 1.241, and the heat transfer efficiency was increased by 24.1%.*

Key words*: self-excited oscillation, pulsating flow, enhanced heat transfer, large eddy simulation*

Introduction

In many engineering fields, in order to improve the heat transfer efficiency, the fluid-flow near the wall of pipe-line has always been one of the focuses of attention. The flow structure near the wall was studied by Kline *et al.* [1], Rafiee and Rahimi [2]. The results revealed that many macroscopic characteristics of the flow, such as the generation and transport of turbulence, the change of resistance, heat transfer, energy transport and dissipation, were related to the coherent structure of the wall boundary-layer. Therefore, changing the large-scale coherent structure in the boundary-layer can increase the turbulence intensity of the fluid, so as to enhance the heat transfer.

* Corresponding author, e-mail: zhwang@wust.edu.cn

Due to the good performance of self-excited oscillation in heat transfer, researchers are now trying to explore the influence of chamber structure parameters on heat transfer performance. Colucci and Viskanta [3] reports results on the effects of hyperbolic nozzle geometry on the local heat transfer coefficients for confined impinging air jets. A thermochromatic liquid-crystal technique is used to visualize and record isotherms on a uniformly heated impingement surface. Experiments are conducted at low nozzle-to-plate spacings ($0.25 < H/D < 6.0$) and Reynolds numbers in the range of 10000-50000 for two different confined, hyperbolic nozzles. They concluded that the local heat transfer coefficients of confined jets are more sensitive to Reynolds number and nozzle-to-plate spacing in comparison unconfined jets. Chiriac and Ortega [4] reported results on heat transfer distribution of a confined slot jet impinging on an isothermal surface for steady and unsteady flows. After averaging over a long time, they concluded that the unsteady flow affects the heat transfer and broadens the extent of cooling, as compared to the steady flow. Liu *et al.* [5] investigated the effects of Reynolds number, Grashof number, and nozzle-to-plate spacing on transient convective heat transfer of a round jet impinging on a confined circular disk. They suggested empirical correlations for calculating transient heat transfer characteristics of the disks.

Changing the channel structure can control the flow pattern of turbulent boundary-layer [6, 7]. Changing the surface of the channel wall can increase the turbulence intensity in the fluids, and improve the flow and heat transfer characteristics of the wall. Liu *et al.* [8] investigated the influence of the improved flow channel structure of plate fin heat exchanger in the fluid-flow in the heat exchanger. The results showed that the improved flow channel structure can significantly enhance the turbulent performance of the fluid in the heat exchanger and improve the heat exchange efficiency of the heat exchanger. Wang *et al.* [9] investigated the flow and heat transfer of small-scale slotted cylindrical vortex generator. The results showed that the interaction between Karman vortex wake and wall boundary-layer can change the coherent structure of turbulent boundary-layer obviously, and the best heat transfer efficiency was obtained when the gap ratio was 2.0. Fan *et al.* [10] investigated the characteristics of heat transfer, flow resistance. The results showed that the increase of turbulence intensity can accelerate the mixing of fluids. Promvonge and Eiamsa-Ard [11] investigated the heat transfer characteristics of uniform heat flow. The results showed that the heat transfer efficiency of conical tube and stud tube was increased by 278% and 206%, respectively. Skullong *et al.* [12] studied the enhanced convective heat transfer in a heated circular tube. The aim at using the pw-xt insert was to produce streamwise-vortex flows, which can reduce the thickness of thermal boundary layer and increase fluid mixing of the flow. Hu *et al.* [13] studied the influence of self-excited oscillation backflow vortex disturbance effect on heat transfer. The results showed that the backflow vortex increased the turbulence intensity of the fluid, and the heat transfer efficiency was increased by 23%.

Biswas *et al.* [14] studied the heat transfer characteristics of finned tube heat exchangers and plate-fin heat exchangers. The results showed that the vortex generator can increase the intensity of turbulence in fluids and improve the heat transfer efficiency of the heat exchange surface. Deshmukh and Vedula [15] studied the turbulent local heat transfer coefficient and average pressure drop in a circular tube. The results showed that the vortex generator can increase the turbulence intensity of the fluid, and the Nusselt value was about 150-500% higher than the corresponding smooth tube value. Skullong *et al.* [16] studied the turbulent flow and heat transfer characteristics in the channel with combined wavy-rib and groove turbulators. Increasing the intensity of turbulence was conducive to improving the heat transfer efficiency. Liang *et al.* [17] studied the heat transfer enhancement and flow structure of vortex generator. The results showed that the vortex generator can produce longitudinal and transverse vortices and increase the turbulence intensity in the fluids. High heat transfer and low pressure drop were obtained. Zhang *et al.* [18] studied the heat transfer and pressure drop in helically coiled tube with spherical corrugation. The results showed that the vortex caused by the corrugated structure can destroy the flow boundary-layer, increase the turbulence intensity of the flow. The performance evaluation index PEC value can reach 1.56.

The pulsating flow has a complicated flow pattern. By controlling its pulsating flow, the purpose of enhancing heat transfer can be achieved to a certain extent [19]. Kurtulmus and Sahin [20] experimentally studied the pulsating flow and heat transfer characteristics of a sinusoidal channel. The results showed that the pulsating flow can increase the intensity of turbulence in fluids and enhance the heat exchange. Khosravi-Bizhaem *et al.* [21] used spiral coils to conduct experimental research on heat transfer and pressure drop. The results showed that compared with the steady pulsating flow, the convective heat transfer was increased by 39%. Jin *et al.* [22] studied the enhancement of heat transfer by pulsating flow in triangular grooves. The PIV results showed that the pulsating flow increaseed the intensity of turbulence in the fluids, and the heat transfer efficiency was increased by 350%. Yoshikawa *et al.* [23] studied the influence of inlet pulsation on the flow in the channel. The research results showed that the air-flow had a greater influence on the flow in the channel, which strengthened the heat transfer on the wall. Lee and Lee [24] studied the influence of self-oscillation nozzle structure on the enhancement of heat transfer. The results showed that the turbulence intensity produced by the self-excited oscillation nozzle structure was higher, so the heat transfer efficiency was higher than that of the traditional nozzle. Zheng *et al.* [25] studied the turbulent flow structure and heat transfer characteristics in pulsating rib-shaped channels. The results showed that the thermal performance increased with the increase of the pulsation amplitude and frequency. Yang *et al.* [26] studied the distribution of secondary flow and Nusselt number in multi-ribbed flow channels under pulsating flow and steady flow. The results showed that the time-average Nusselt number on the fin surface of the pulsating flow was significantly higher than that of the steady flow. Akdag *et al.* [27] investigated heat transfer and pressure drop characteristics of CuO-water nanofluid-flow under pulsating inlet conditions. The results showed that under the condition of pulsating flow, the heat transfer performance was significantly improved due to the increase of thermal conductivity and the use of nanoparticles.

The aforementioned literatures showed that many studies increase the turbulence intensity in the channel by generating pulsating flow and changing the structure of the channel, and accelerate the disturbance in the fluids, so as to improve the heat transfer efficiency. According to the Helmholtz cavity model, pulsating flow can be formed in the self-excited oscillating hot runner. The *variable pulsating flow* characteristics of self-excited oscillation chamber can effectively improve the mixing of fluids in hot runner, increase the turbulence intensity in fluids and improve the heat transfer efficiency. In this work, the influence of disturbance effect of pulsating flow in the self-excited oscillating hot runner on the heat transfer was studied. The instantaneous velocity, wall shear stress, boundary-layer thickness and Nusselt number number of hot runner section under different structural parameters were studied. Finally, the comprehensive evaluation factor, *PI*, was established to analyze the heat transfer efficiency in hot runner. The research results will provide theoretical and scientific basis for the design of self-excited oscillation pulsating flow heat exchanger.

Disturbance effect of pulsating flow in self-excited oscillation hot runner

When the jet enters a round tube, the fluid-flow is laminar due to the simple structure of the round tube. Under the action of fluid viscosity, a boundary-layer can be formed near the wall. As the main flow moves downward, the intensity of turbulence in hot runner decreases continuously. The mixing of fluids is weak and the heat exchange efficiency is getting worse.

In order to improve the heat transfer efficiency, increasing the intensity of turbulence in the fluids and reducing the boundary-layer thickness was one of the effective methods to improve the heat transfer efficiency. Figure 1 showed a schematic diagram of fluid-flow under the disturbance effect of pulsating flow in a self-excited oscillation hot runner. After the fluid entered the pipe, unlike the round pipe, the pulsating flow was generated at the axis center of the hot runner. The pulsating flow can disturb the fluid at the axis center and strengthen the intensity of turbulence in the fluids. The right side of fig. 1 was a schematic diagram of the flow velocity in the pipe when the pulsating flow existed. Under the disturbance effect of pulsating flow, the velocity direction of the fluid near the axis center of hot runner was opposite to that of the main flow. It will strengthen the heat exchange between the fluid and the wall of the mainstream area and improve the heat exchange efficiency.

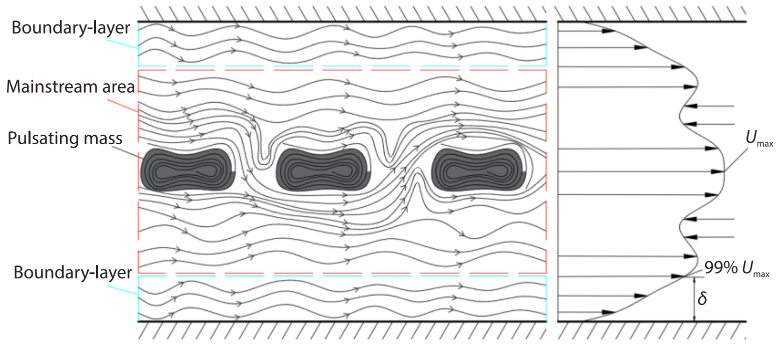

Figure 1. Disturbance effect of pulsating flow in self-excited oscillation hot runner

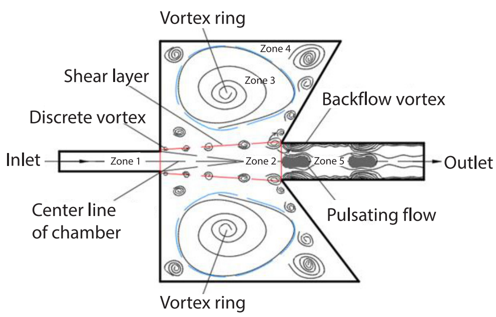

Figure 2. Schematic diagram of the formation of pulsating flow in self-excited oscillation

The U_{max} is the maximum velocity of the mainstream and δ is the boundary-layer thickness.

The vorticity of self-excited oscillation chamber was expressed by velocity field. As shown in fig. 2, the unstable shear layer was surrounded by an axisymmetric discrete vortex ring, which divided the self-excited oscillation chamber into five regions: Zone 1 is the upstream flow channel, Zone 2 with red frame is the shear layer and downstream channel, Zone 3 with blue frame is the large vortex convergence area, Zone 4 is the separation zone, and Zone 5 is the hot runner zone.

The self-excited oscillation with a special structure can form a pulsating flow in the hot runner, which is different from the flow in a round tube. The thickness of viscous bottom layer on the wall of the cavity is thin by the shear layer produced by the self-excited oscillation chamber. The formation mechanism of pulsating flow in self excited oscillation hot runner was shown in fig. 2. When the discrete vortices in the shear layer moved to the collision angle of the cavity, the blocking of the collision angle will cause the shear layer to split into two parts. Some feeded back to the upper part of the chamber along the collision wall and eventually gathered in the middle of the chamber. The other part flowed along the downstream wall and formed a backflow vortex near the wall. The fluid at the axis center formed pulsating flow under the squeezing action of backflow vortices. Therefore, it can be seen that the formation of pulsating flow was closely related to the upstream and downstream pipe diameter ratio and cavity diameter ratio, which can determine the disturbance effect of pulsating flow. In this paper, the disturbance effect of pulsating flow in the hot runner was studied.

The boundary-layer thickness is defined as δ. Since the heat transfer between the fluid and the wall is convective, the heat transfer formula can be obtained:

$$Q = \frac{t_1 - t_2}{\dfrac{\delta}{\lambda A}} = \frac{\Delta t}{R} \tag{1}$$

where δ is the thickness of the velocity boundary-layer and R – the thermal resistance.

Since fluid velocity boundary-layer thickness is defined as the distance from the wall to 99% of the maximum incoming velocity, the relationship between the velocity and the boundary-layer is expressed:

$$\frac{\partial u}{\partial y} = \frac{0.99U}{\delta} \tag{2}$$

It shows that the boundary-layer thickness is inversely proportional to the velocity gradient, and the larger the velocity gradient, the smaller the boundary-layer.

The relevant parameters are defined:

$$\mathrm{Nu}_x = \frac{h_\mathrm{x} d_2}{\lambda} \tag{3}$$

$$\overline{\mathrm{Nu}} = \frac{1}{l_2}\int_0^{l_2} \mathrm{Nu}_x \mathrm{d}x \tag{4}$$

where Nu_x is the local Nusselt number and h_x – the local surface heat transfer coefficient.

Considering that the fluid-flows near the pipe wall as laminar flow, the wall friction resistance f is defined:

$$f = \tau \pi d_2 l_2 \tag{5}$$

The shear stress per unit area in hot runner of self-excited oscillation is defined:

$$\tau = \mu \frac{\mathrm{d}u}{\mathrm{d}y} \tag{6}$$

$$\overline{f} = \frac{1}{A}\int \tau_\mathrm{x} \mathrm{d}A \tag{7}$$

where μ is the internal friction coefficient, $\mathrm{d}\mu/\mathrm{d}y$ – the velocity gradient, and $\overline{f}$ – the average wall friction resistance. It can be seen that the shear stress is directly proportional to the velocity gradient. The friction resistance is proportional to the wall shear stress, and the friction resistance is proportional to the velocity gradient, when the diameter and length of the pipe are fixed.

The comprehensive evaluation factor PI is used to characterize the heat transfer performance of the self-excited oscillation hot runner:

$$PI = \frac{\overline{\mathrm{Nu}} / \overline{\mathrm{Nu}_0}}{\left(\overline{f} / \overline{f_0}\right)^{1/3}} \tag{8}$$

Numerical model

Physical model and boundary conditions

The pulsating flow of hot runner in the self-excited oscillation chamber is a flow composed of vortices of different structures and scales, and has the characteristics of unsteady and irregular. The key structural parameters of the self-excited oscillation chamber are as shown in fig. 3: diameter of upstream pipe inlet, d_0, diameter of upstream pipe outlet, d_1, diameter of downstream pipe, d_2, length of upstream inlet channel, l_1, length of downstream inlet channel, l_2, conical contraction angle, α_1, conical diffusion angle, α_2, length of chamber, L, and diameter of chamber, D.

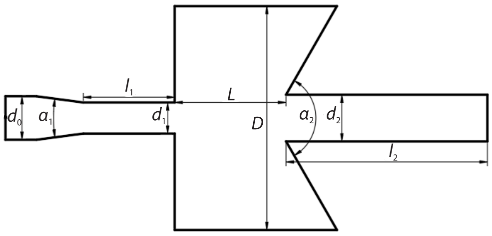

Figure 3. Structure of self-excited oscillation chamber

According to the optimum range of the design parameters of Helmholtz resonator provided in reference [28], the design parameters of the cavity are as shown in tab. 1.

Table 1. Main structural parameters of self-excited oscillation chamber

Main structure parameters	Value [mm]
Diameter of upstream pipe inlet/diameter of upstream pipe outlet, d_0/d_1	1.4
Length of chamber/diameter of chamber, L/D	0.45-0.65
Diameter of downstream pipe/diameter of upstream pipe outlet, d_2/d_1	0.8-1.6
Conical contraction angle, α_1	15°
Conical diffusion angle, α_2	120°

In this work, we refer to our previous research work [29]. In self-excited oscillation chamber, the inlet pressure is 5000 Pa, and the relative pressure of the downstream outlet is 0. The inlet temperature is 293.15 K. The wall temperature is 343.15 K, and the outlet temperature is 313.15 K. The second order implicit scheme is used for the time term, and the second order upwind scheme is used for the convection and diffusion terms. The time step is 10^{-4}. The convergence residuals are 10^{-6} and the residuals of physical quantities fluctuate stably.

Governing equations

The structural changes of unsteady large-scale vortices are captured and the periodic instantaneous vortex structure change in the self-excited oscillation chamber is solved using the large eddy simulation (LES). In the unsteady Navier-Stokes equations, the small vortices are represented by a subgrid scale model with additional stress terms [30]. On the basis of filtering, the continuity equation, momentum equation of incompressible flow are obtained:

$$\frac{\partial \overline{u}_i}{\partial x_i} = 0 \tag{9}$$

$$\frac{\partial}{\partial t}\left(\rho \overline{u}_i\right) + \frac{\partial}{\partial x_j}\left(\rho \overline{u}_i \overline{u}_j\right) = -\frac{\partial \overline{p}}{\partial x_i} - \frac{\partial \tau_{ij}}{\partial x_j} + \frac{\partial}{\partial x_j}\left(\mu \frac{\partial \overline{u}_i}{\partial x_j}\right) \tag{10}$$

where t is the time, u – the velocity component, μ – the dynamic viscosity coefficient, α – the conduction temperature coefficient, ρ – the density, and τ_{ij} – the subgrid scale stress:

$$\tau_{ij} = \rho\left(\overline{u_i u_j} - \bar{u}_i \bar{u}_j\right) \tag{11}$$

The sub-grid tensor accounts for the averaged sub-grid part of the velocity field. Closure of the model requires a modelling of that tensor. To that purpose, Small-scale vortex is modeled using the sub-grid scale model proposed by [31]:

$$\tau_{ij} - \frac{1}{3}\tau_{kk}\delta_{ij} = 2\mu_t \overline{S_{ij}} \tag{12}$$

where τ_{kk} is the isotropic sub-grid stress, δ_{ij} – the Kroneker symbol, when $i = j$, $\delta_{ij} = 1$, when $i \neq j$, $\delta_{ij} = 0$, Sij – the filtered deformation rate tensor and μ_t – the eddy viscosity coefficient:

$$\mu_t = \left(C_s \Delta_i\right)^2 \left|\bar{S}\right| \tag{13}$$

$$\overline{S_{ij}} = \frac{1}{2}\left(\frac{\partial \bar{u}_i}{\partial x_j} + \frac{\partial \bar{u}_j}{\partial x_i}\right) \tag{14}$$

where Δi is the mesh size along the i-axis, C_s – the sub-grid scale stress constant (taken here to be 0.1 as in [32]), and $\bar{S}$ – the second invariant of the shear rate tensor.

Model verification

Grid independence test

The quadrilateral grid was used to mesh computational domain. The non-slip boundary condition was selected. After 0.5 second, the average velocity and upstream and downstream pressure drop under six different structured mesh numbers were calculated, respectively, and the mesh independence verification diagram shown in fig. 4 was obtained. The results showed that with the increase of the number of grids, the average velocity in the hot runner and the pressure drop tended to be stable, indicating that the change of grid had little effect on the calculation. Considering the calculation time and accuracy, the grid model with 296360 grids was determined.

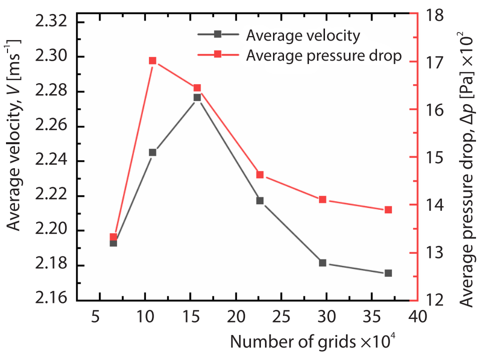

Figure 4. Grid independence verification

Turbulence model verification

The main forms of turbulence in the shear layer of self-excited oscillating jet are the merging, movement and shedding of vortex structures. The LES is a kind of turbulence numerical simulation method between DNS and Reynolds average, which can capture the structural changes of unsteady large-scale vortices. In the validation process of turbulence model, the inlet pressure is set at 12000pa. The Nusselt number curve was compared with the results of [33] at different Reynolds numbers. It can be seen from tab. 2 that numerical results were in good agreement with the literature results, and the error was less than 2%. It showed that the numerical simulation results were reasonable:

$$\mathrm{Nu} = 0.23\,\mathrm{Re}^{0.8}\,\mathrm{Pr}^{0.4} \tag{15}$$

Table 2. Comparison of Nusselt number curve and literature under different Reynolds numbers

Inlet [Pa]	Outlet [Pa]	Grid number	Prandtl number	Reynolds number	Present study/ Nusselt number	[32] Nusselt number	Error [%]
12000	0	296360	0.87	56000	135	137	–1.46
12000	0	296360	0.83	58000	139	138	0.72
12000	0	296360	0.83	60000	143	142	0.7
12000	0	296360	0.86	62000	146	148	–0.48
12000	0	296360	0.87	64000	150	152	–1.32
12000	0	296360	0.83	66000	155	153	1.31

Results and discussion

Formation of pulsating flow in self-excited oscillating hot runner

The shear layer is formed after the jet enters the chamber from the inlet. Assuming that the upstream inlet pressure is 5000 Pa, fig. 5 showed the change of instantaneous velocity at different positions at different times of a pulsating flow cycle in the chamber. When $t = T/4$, shear layer reached the wall collision angle. When $t = T/2$, the discrete vortex was divided into two parts by the wall collision angle. One part moved upstream along the wall, and the other

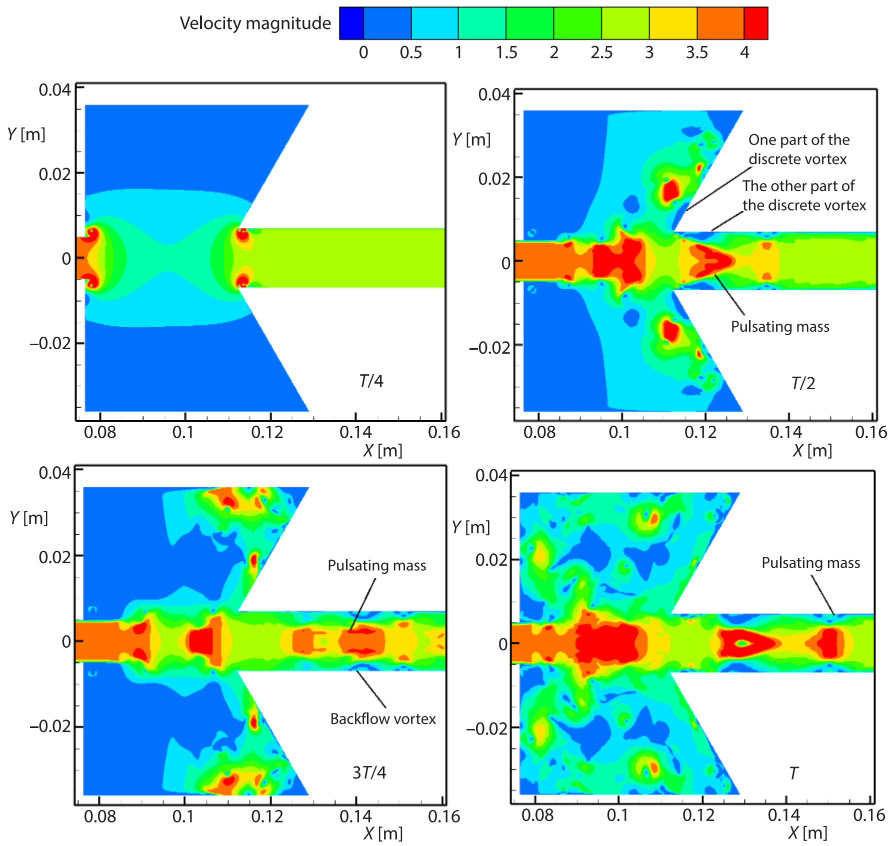

Figure 5. Cloud diagram of velocity in self-excited oscillation chamber in one cycle

part flowed downstream along the main flow direction. Due to the speed difference between the mainstream velocity and the velocity of the fluid near the wall, the fluid near the wall formed a backflow vortex during the flow process. The pulsation mass at the axis center was formed under the squeezing action of the backflow vortex. When $t = 3T/4$, It can be seen that the pulsation mass moved to $x = 0.14$ m at this time. The size and intensity of the pulsation mass increased. When $t = T$, the separated discrete vortices moved to the shear layer and strengthened the generation of new discrete vortices at the shear layer.

The evolution of the pulsating flow in the self-excited oscillating hot runner

After the fluid-flows through the self-excited oscillation chamber, due to the strong shear stress and the vertical disturbance caused by the wall collision, the self-excited oscillation pulsating flow was formed at the axis center of the hot runner. Figure 6 showed the evolution of the hot runner velocity in a pulsating flow in a cycle. When $t = T/4$, the pulsation mass at the axis center was formed under the squeezing action of the backflow vortex. The velocity of pulsation mass reached 4.4 m/s. The fluid velocity near the pulsating flow was 1.9-2.5 m/s. When $t = T/2$, the pulsating flow moved to $x = 0.14$ m. The central flow velocity after squeezing reached 5 m/s. The fluid velocity near the pulsation mass was 2.5-3.1 m/s. When $t = 3T/4$, the pulsating flow moved to $x = 0.16$ m. The velocity near the pulsating flow was 2.5-3.8 m/s, and

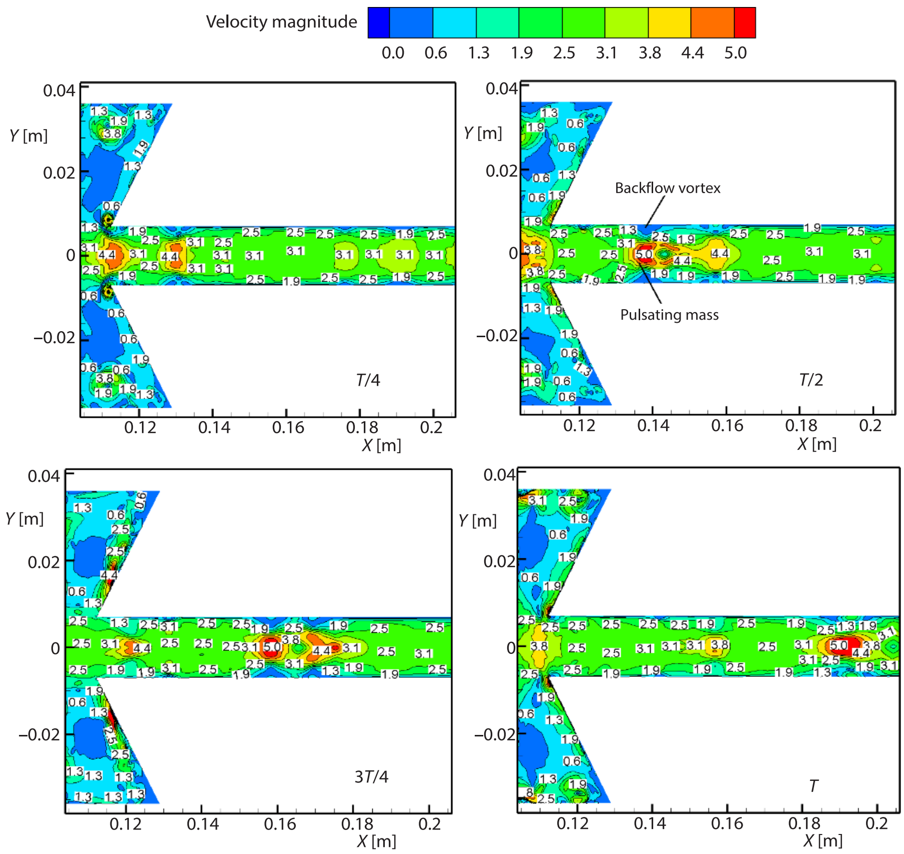

Figure 6. The evolution of pulsating flow in the self-excited oscillating hot runner

the velocity and range of action near the pulsating flow were increasing. When $t = T$, the pulsating flow moved to $x = 0.18$, and the velocity near the pulsating flow was 3.8-4.4 m/s. The action area of pulsating flow and the action range of the mainstream area were increasing. It can be seen from the velocity diagram that the action range of the pulsating flow increased gradually with the mainstream flow. The distance between pulsating flowes was not exactly the same. Due to the viscous interaction between the fluids, the released energy presents *variable pulsating flow* after reaching the hot runner. The formation of *variable pulsating flow* can effectively increase the disturbance of the fluid in the hot runner, and make the heat transfer between the fluid at the axis and the wall more sufficient.

The velocity at the axis center and wall shear stress in the self-excited oscillation hot runner

It can be seen from the velocity streamline diagram that after the fluid enters the self-excited oscillation chamber, pulsating flow is formed in the hot runner. Figure 7(a) showed the velocity curve of hot runner axis center position under different d_2/d_1. When $d_2/d_1 = 1$, the velocity range was 2.66-3.88 m/s. It can be seen that the maximum speed was 3.88 m/s. When $d_2/d_1 = 1.2$, the speed range was 2.01-4.81 m/s. The overall velocity at the axis center increased, indicating that the disturbance effect of pulsating flow in hot runner was better. When $d_2/d_1 = 1.4$, the velocity range at the axis center was 2.36-5.12 m/s, and the overall velocity fluctuation increased again. Due to the better structure of the d_2/d_1, the pulsating flow reaching the downstream hot runner intensified the fluid disturbance at the axis center. When $d_2/d_1 = 1.6$, the velocity range at the axis center was 1.51-4.79 m/s, and the overall velocity range decreased. When $d_2/d_1 = 1.8$, the velocity range at the axis center was 1.7-4.3 m/s. The energy of the pulsating flow was low and the disturbance effect was poor. It can be seen from the aforementioned that the velocity at the axis center position fluctuated periodically and increased gradually. When $d_2/d_1 = 1.4$, the disturbance effect of pulsating flow and the heat transfer efficiency was the best.

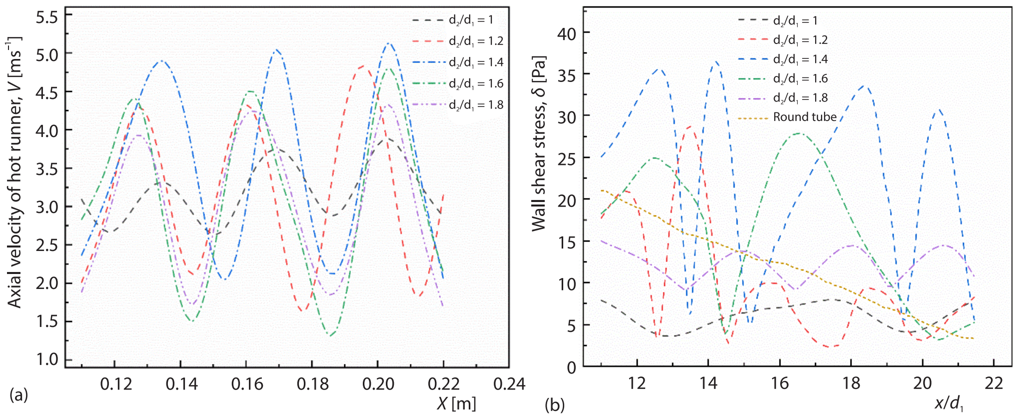

Figure 7. Velocity at the axis center of the hot runner (a) and wall shear stress (b) under different upstream and downstream pipe diameter ratios

Wall shear stress was caused by surface friction. The greater the wall shear stress was, the greater the friction and pressure drop were. The wall shear stress changes under different d_2/d_1 were shown in fig. 7(b). In the hot runner without self-excited oscillation, the wall shear stress decreased steadily with the change of the axis center position. In the self-excited oscillation hot runner, when $d_2/d_1 = 1$, the wall shear stress was 2.2-7.8 Pa. The wall shear stress was lower than that of a round tube, and the heat exchange efficiency was poor. When $d_2/d_1 = 1.2$, the wall shear stress first increased and then tended to fluctuate, showing periodicity. The wall shear stress varied in the range of 2.5-28 Pa. When $d_2/d_1 = 1.4$, the wall shear stress first increased and then tended to fluctuate periodically, reaching a maximum of 36.4 Pa. The fluid at the axis center formed a pulsation mass under the squeezing action of the backflow vortex. The pulsating flow disturbed the nearby fluid, and the flow velocity of the fluid slowed down, which leaded to the increase of the velocity gradient and the wall shear stress. When $d_2/d_1 = 1.6$, 1.8, the wall shear stress decreased. The wall shear stress was lower than that of the horizontal round pipe, and the heat transfer was poor. It can be seen from the aforementioned that with the increase of d_2/d_1, the wall shear stress first increased and then decreased, and the wall heat transfer first increased and then decreased. When $d_2/d_1 = 1.4$, the heat transfer efficiency was the best.

Boundary-layer thickness and Nusselt number in self-excited oscillation hot runner

Under the squeezing action of the backflow vortex, the fluid at the axis center formed a pulsating flow. The ratio of cavity diameter can determine the strength of the pulsating flow in the hot runner. When $t = 0.5$ second, the boundary-layer thickness was extracted. The boundary-layer thickness under different L/D were shown in fig. 8(a). In the hot runner without self-excited oscillation, the boundary-layer thickness keeped increasing steadily. In the self-excited oscillating hot runner, when $L/D = 0.45$, the boundary-layer thickness was at least 1.11 mm. When $L/D = 0.5$. Under the action of the pulsating flow, the minimum boundary-layer thickness reached 0.718 mm. When $L/D = 0.55$, it can be seen that the boundary-layer thickness decreased again, reaching a minimum of 0.392 mm. It showed that the pulsating flow was strengthening, and the disturbance effect of pulsating flow was more obvious. When $L/D = 0.6$, 0.65, the minimum boundary-layer thickness reached 0.477 mm and 0.539 mm, respectively. It can be seen that with the gradual increase of L/D, the the boundary-layer thickness first decreased and then increased, and the heat transfer first increased and then decreased. When $L/D = 0.55$, the boundary-layer thickness was at least 0.392 mm, and the heat transfer efficiency was the best.

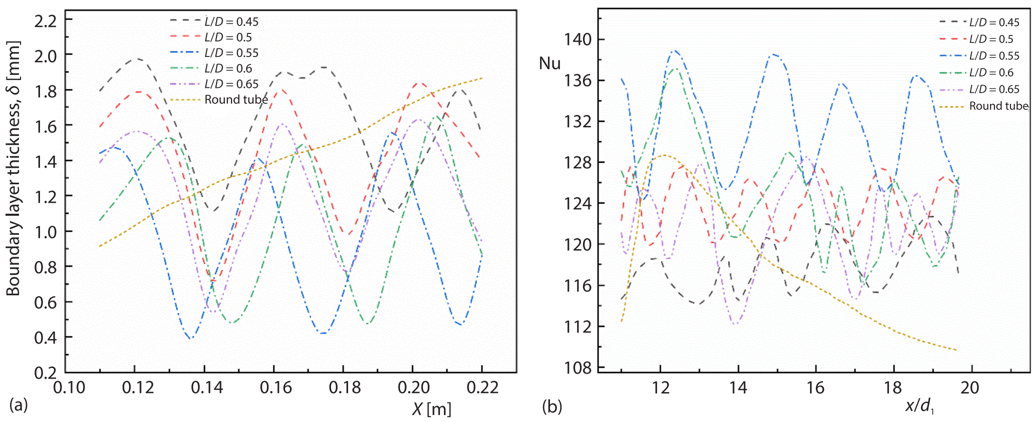

Figure 8. Boundary-layer thickness of hot runner (a) and Nusselt number curve of wall (b) under different cavity diameter ratio

The wall Nusselt number can effectively characterize the heat exchange between the fluid and the wall. The Nusselt number curve distribution under different L/D was shown in fig. 8(b). When L/D = 0.45, the Nusselt number gradually decreased and the minimum was 114. The heat transfer was poor. When L/D = 0.5, the maximum Nusselt number was 127. The Nusselt number fluctuated periodically. When L/D = 0.55, the Nusselt number increased significantly, reaching a maximum of 138. The Nusselt number can present periodic fluctuations, and the heat transfer was the best at this time. It can be explained that the pulsating flow at the axis center of the hot runner enhanced the disturbance in fluids. When L/D = 0.6, 0.65, the Nusselt number was decreasing. It showed that the L/D was too large, and the hot runner failed to form an effective pulsation mass. It can be explained from the aforementioned that as the cavity diameter ratio increased, the Nusselt number first increased and then decreased. When the L/D = 0.55, the Nusselt number reached the maximum at this time, and the heat transfer efficiency was the best.

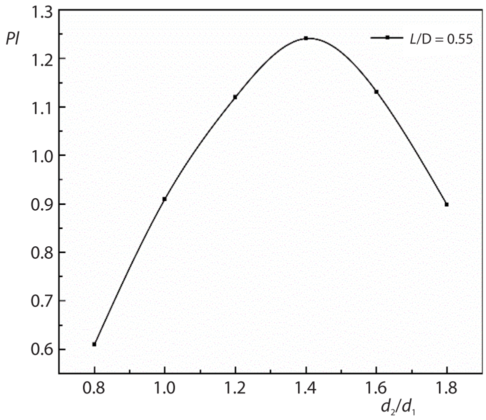

Figure 9. The change curve of *PI* under different d_2/d_1

Comprehensive evaluation factor PI

The comprehensive evaluation factor PI is used to characterize the heat transfer performance of the self-excited oscillation chamber pipe. The $PI > 1$ indicates that the increase of heat transfer is greater than that of flow resistance, and $PI < 1$ indicates that the increase of heat transfer is less than that of flow resistance. Figure 9 showed the variation curve of PI under different d_2/d_1. It can be seen from fig. 9 that the value of PI showed a trend of first increasing and then decreasing with the increase of d_2/d_1. When d_2/d_1 = 1.2, 1.4, and 1.6, PI was greater than 1, indicating that the heat transfer efficiency was better. When d_2/d_1 = 1.4, the maximum PI was 1.241, and the heat transfer performance was the best. Compared with ordinary horizontal round pipes, the comprehensive evaluation factor PI can be increased by 24.1%.

Conclusions

In this paper, LES was used to analyze the formation and periodic evolution of pulsating flow in the self-excited oscillating hot runner. The heat transfer characteristics of hot runner were studied under different d_2/d_1 and L/D. The main conclusions were are as follows.

- The pulsating flow had a strong disturbing effect and accelerated the heat exchange on the fluid at the axis center. As the pulsating flow moved downstream with the main flow, the size and intensity of the disturbance effect of the pulsating flow gradually increased.
- The pulsation mass presented a periodic *variable pulsation mass* characteristic. When $t = T/4$, the discrete vortex collided with the collision wall. When $t = T/2$, after the discrete vortex passed through the collision angle, one part of the discrete vortex moved upstream. The other part flowed downstream along the main flow direction form a backflow vortex, and the fluid at the axis center formed a pulsating flow under the squeezing action of the backflow vortex. When $t = T$, the discrete vortex moved to the shear layer. The generation of new discrete vortices in the shear layer was enhanced, and the next period of reverse disturbance occured with the colliding wall.
- When the d_2/d_1 is 1-1.8, the wall shear stress first increased and then decreased, and the wall heat transfer efficiency first increased and then decreased. The maximum wall shear stress

was 36.4 Pa. When the L/D was 0.45-0.65, the boundary-layer thickness first decreased and then increased, and the heat transfer efficiency first increased and then decreased. The minimum boundary-layer thickness was 0.392 mm and the maximum Nu = 138. When $d_2/d_1 = 1.4$ and $L/D = 0.55$, the maximum comprehensive evaluation factor was 1.241, and the heat transfer efficiency was increased by 24.1%.

Acknowledgment

This work was supported by the National Natural Science Foundation of China (Grant No. 51875419).

Nomenclature

D – diameter of chamber, [m]
d_0 – diameter of upstream pipe inlet, [m]
d_1 – diameter of upstream pipe outlet, [m]
d_2 – diameter of downstream pipe, [m]
f – friction, [N]
$\overline{f}$ – average friction, [N]
$\overline{f}_0$ – round pipe average friction force, [N]
h – heat transfer coefficient, [Wm^{-2}K^{-1}]
L – length of chamber, [m]
l_1 – length of upstream inlet pipe, [m]
l_2 – length of downstream inlet pipe, [m]
Nu – Nusselt number (= hd/λ), [–]
$\overline{\text{Nu}}$ – mean Nusselt number, [–]
$\overline{\text{Nu}}_0$ – round pipe average Nusselt number, [–]
Δp – pressure drop, [Pa]
PI – comprehensive evaluation factors, [–]
R – thermal resistance, [kW^{-1}]
Re – Reynolds number (=$\rho UDh/\mu$), [–]
T – temperature, [K]
t – time, [s]
U – main flow velocity, [ms^{-1}]

Greek symbols

α_1 – conical contraction angle, [°]
α_2 – conical diffusion angle, [°]
δ – boundary-layer thickness, [m]
λ – convective heat transfer coefficient, [–]
μ – internal friction factor, [Nsm^{-2}]
ρ – density, [kgm^{-3}]
τ – shear stress, [Nm^{-2}]

Subscirpts

max – maximum
x – local

References

[1] Kline, S. J., *et al.*, The Structure of Turbulent Boundary-layers, *Journal of Fluid Mechanics*, *30* (2006), 4, pp. 741-773
[2] Rafiee, S. E., Rahimi, M., The 3-D Simulation of Fluid-flow and Energy Separation Inside a Vortex Tube, *Journal of Thermophysics and Heat Transfer*, *28* (2014), 1, pp. 87-99
[3] Colucci, D. W., Viskanta, R., Effect of Nozzle Geometry on Local Convective Heat Transfer to a Confined Impinging Air Jet, *Experimental Thermal and Fluid Science*, *13* (1996), 1, pp. 71-80
[4] Chiriac, V. A., Ortega, A., A Numerical Study of the Unsteady Flow and Heat Transfer in a Transitional Confined Slot Jet Impinging on an Isothermal Surface, *International Journal of Heat and Mass Transfer*, *45* (2002), 6, pp.1237-1248
[5] Liu, L. K., *et al.*, Transient Convective Heat Transfer of Air Jet Impinging on a Confined Ceramic-Based MCM, *Journal of Electronic Packaging*, *126* (2004), 1, pp. 159-172
[6] Wang, J. S., *et al*., Heat Transfer Enhancement Mechanism of Semi Elliptical Vortex Generator (in Chinese), *Chinese Journal of Mechanical Engineering*, *42* (2006), 5, pp. 160-164
[7] Ye, Q. L., *et al*., Experimental Study on Heat Transfer Enhancement and Pressure Drop Characteristics of Inclined Semi Elliptical Cylindrical Vortex Generator (in Chinese), *Chinese Journal of Mechanical Engineering*, *46* (2010), 16, pp. 162-169
[8] Liu, J. C., *et al*., Structure Improvement and Fluid-flow Performance Analysis of Plate Fin Heat Exchanger (in Chinese), *Chinese Journal of Mechanical Engineering*, *50* (2014), 18, pp. 167-176
[9] Wang, J. S., *et al*., Flow and Heat Transfer Characteristics of Bluff Body Turbulence in Turbulent Boundary-Layer (in Chinese), *Chinese Journal of Mechanical Engineering*, *51* (2015), 24, pp. 168-176
[10] Fan, A., *et al*., A Numerical Study on Thermo-hydraulic Characteristics of Turbulent Flow in a Circular Tube Fitted with Conical Strip Inserts, *Applied Thermal Engineering*, *31* (2011), 15, pp. 2819-2828
[11] Promvonge, P., Eiamsa-Ard, S., Heat Transfer Enhancement in a Tube with Combined Conical-nozzle Inserts and Swirl Generator, *Energy Conversion and Management*, *47* (2006), 18, pp. 2867-2882

[12] Skullong, S., *et al*., Thermal Behaviors in a Round Tube Equipped with Quadruple Perforated-delta-Winglet Pairs, *Applied Thermal Engineering*, *115* (2017), Mar., pp. 229-243
[13] Hu, G. Q., *et a*l., Study on Heat Transfer in Self-excited Oscillation with Backflow Vortex Disturbance Effect, *Journal of Thermophysics and Heat Transfer*, *5* (2021), Feb., pp. 1-11
[14] Biswas, G., *et al.*, Augmentation of Heat Transfer by Creation of Streamwise Longitudinal Vortices Using Vortex Generators, *Heat Transfer Engineering*, *33* (2012), 4, pp. 406-424
[15] Deshmukh, P. W., Vedula, R. P., Heat Transfer and Friction Factor Characteristics of Turbulent Flow Through a Circular Tube Fitted with Vortex Generator Inserts, *International Journal of Heat and Mass Transfer*, *79* (2014), Dec., pp. 551-560
[16] Skullong, S., *et al*., Thermal Performance of Turbulent Flow in a Solar Air Heater Channel with Rib-groove Turbulators, *International Communications in Heat and Mass Transfer*, *50* (2014), Jan., pp. 34-43
[17] Liang, G., *et al*., Numerical Study of Heat Transfer and Flow Behavior in a Circular Tube Fitted with Varying Arrays of Winglet Vortex Generators, *International Journal of Thermal Sciences*, *134* (2018), Dec., pp. 54-65
[18] Zhang, C. C., *et al*., Numerical Investigation of Heat Transfer and Pressure Drop in Helically Coiled Tube with Spherical Corrugation, *International Journal of Heat and Mass Transfer*, *113* (2017), Oct., pp. 332-341
[19] Yu, J. C., Li, Z. X., Numerical Analysis of Convective Heat Transfer Enhancement by Laminar Pulse Flow in Circular Tubes with Annular Inner Fins (in Chinese), *Journal Tsing University*, *45* (2005), 8, pp. 1091-1094
[20] Kurtulmus, N., Sahin, B., Experimental Investigation of Pulsating Flow Structures and Heat Transfer Characteristics in Sinusoidal Channels, *International Journal of Mechanical Sciences*, *167* (2020), 105268
[21] Khosravi-Bizhaem, H., *et al*., Heat Transfer Enhancement and Pressure Drop by Pulsating Flow through Helically Coiled Tube: An Experimental Study, *Applied Thermal Engineering*, *160* (2019), 114012
[22] Jin, D. X., *et al*., Effects of the Pulsating Flow Agitation on the Heat Transfer in a Triangular Grooved Channel, *International Journal of Heat and Mass Transfer*, *50* (2007), 15, pp. 3062-3071
[23] Yoshikawa, H., *et a*l., Effects of Pulsation on Separated Flow and Heat Transfer in Enlarged Channel, *Journal of Thermal Sciences*, *20* (2011), 1, pp. 70-75
[24] Lee, J., Lee, S. J., The Efect of Nozzle Configuration on Stagnation Region Heat Transfer Enhancement of Axisymmetric Jet Impingement, *International Journal of Heat and Mass Transfer*, *43* (2000), 18, pp. 3497-3509
[25] Zheng, D., *et al*., The Effect of Pulsating Parameters on the Spatiotemporal Variation of Flow and Heat Transfer Characteristics in a Ribbed Channel of a Gas Turbine Blade with the Pulsating Inlet Flow, *International Journal of Heat and Mass Transfer*, *153* (2020), 119609
[26] Yang, B., *et al*., Numerical Investigation on Flow and Heat Transfer of Pulsating Flow in Various Ribbed Channels, *Applied Thermal Engineering*, *145* (2018), Dec., pp. 576-589
[27] Akdag, U., *et al*., Heat Transfer in a Triangular Wavy Channel with CuO/Water Nanofluids under Pulsating Flow, *Thermal Science*, *23* (2017), 1, pp. 191-205
[28] Pan, Z. M., Application and Test of Pipe-line Booster in Natural Gas Pipe-line, Ph. D. thesis, Chongqin University, Chongqin, China, 2009
[29] Cheng, Z., *et al*., Multi-Objective Optimization of Self-Excited Oscillation Heat Exchange Tube Based on Multiple Concepts, *Applied Thermal Engineering*, *197* (2021), 117414
[30] Wang, J. S., *et al*., Flow and Heat Transfer Characteristics of Bluff Body Turbulence in Turbulent Boundary-layer (in Chinese), *Chinese Journal of Mechanical Engineering*, *51* (2015), 24, pp. 168-176
[31] Felten, F., *et al*., Numerical modelling of electromagnetically-driven turbulent flows using LES methods, *Applied Mathematical Modelling*, *28* (2004), 1, pp. 15-27
[32] Breuer, M., Pourquie, M., First experiences with LES of flows past bluff bodies, (Eds. W. Rodi, G. Bergeles), *Proceedings*, 3rd Int. Symp. on Engineering Turbulence Modelling and Measurements, Heraklion-Crete, Greece, 1996, Elsevier, Amsterdam, The Netherlands, 1996, pp. 177-186
[33] Davletshin, I. A., *et al*., Convective Heat Transfer in the Channel Entrance with a Square Leading Edge Under Forced Flow Pulsations, *International Journal of Heat and Mass Transfer*, *129* (2019), Feb., pp. 74-85

Paper submitted: June 11 2021
Paper revised: September 23, 2021
Paper accepted: November 16, 2021